

*Spatial interaction among nontoxic
phytoplankton, toxic phytoplankton,
and zooplankton: Emergence in space and time*

Roy, Shovonlal

2008

MIMS EPrint: **2008.78**

Manchester Institute for Mathematical Sciences
School of Mathematics

The University of Manchester

Reports available from: <http://eprints.maths.manchester.ac.uk/>

And by contacting: The MIMS Secretary
School of Mathematics
The University of Manchester
Manchester, M13 9PL, UK

ISSN 1749-9097

Spatial Interaction Among Nontoxic Phytoplankton, Toxic Phytoplankton, and Zooplankton: Emergence in Space and Time

Shovonlal Roy

Received: 24 February 2008 / Accepted: 23 June 2008
© Springer Science + Business Media B.V. 2008

Abstract In homogeneous environments, by overturning the possibility of competitive exclusion among phytoplankton species, and by regulating the dynamics of overall plankton population, toxin-producing phytoplankton (TPP) potentially help in maintaining plankton diversity—a result shown recently. Here, I explore the competitive effects of TPP on phytoplankton and zooplankton species undergoing spatial movements in the subsurface water. The spatial interactions among the species are represented in the form of reaction-diffusion equations. Suitable parametric conditions under which Turing patterns may or may not evolve are investigated. Spatiotemporal distributions of species biomass are simulated using the diffusivity assumptions realistic for natural planktonic systems. The study demonstrates that spatial movements of planktonic systems in the presence of TPP generate and maintain inhomogeneous biomass distribution of competing phytoplankton, as well as grazer zooplankton, thereby ensuring the persistence of multiple species in space and time. The overall results may potentially explain the sustainability of biodiversity and the spatiotemporal emergence of phytoplankton and zooplankton species under the influence of TPP combined with their physical movement in the subsurface water.

Keywords Phytoplankton · Toxin · Allelopathy · Competitive coexistence · Paradox of plankton · Diffusion · Spatial dynamics

1 Introduction

Over many decades, the extreme diversity of phytoplankton and zooplankton species in marine ecosystems has been a topic of interest for numerous theoreticians and experimentalists. To explain how this high diversity of plankton population is maintained in natural waters, a number of mechanisms based on temporal, spatial, and spatiotemporal dynamics

S. Roy (✉)
School of Mathematics, The University of Manchester,
Alan Turing Building, Manchester M13 9PL, UK
e-mail: shovonlal_roy@yahoo.com

have been proposed [e.g., 1–4]. A detailed account of those various mechanisms can be found in Scheffer et al. [5] and Roy and Chattopadhyay [6]. Apart from several physical and biological reasons, the complexity of species interaction, mainly on a spatiotemporal scale, has been identified as a probable reason for the regulation of plankton dynamics (detailed in Medvinsky et al. [7]). However, a specific group of phytoplankton common to most aquatic ecosystems has the special physiological feature of releasing both “toxic” or “allelopathic agents” harmful for the growth of other algae [8, 9]. Observations both *in vitro* and *in situ* have reported the presence of allelopathy among marine algae [e.g., 10–14]. Algal toxicity is known to have a significant impact on phytoplankton–zooplankton interactions [11, 15, 16]. Recently, through an integrated study combining a field observation and mathematical modeling, along with coauthors, I have attempted [e.g., 17–19] to explore the role of toxin-producing phytoplankton (TPP) in determining the dynamics and maintaining diversity of the overall phytoplankton and zooplankton species in the Bay of Bengal. These studies have suggested that the toxic chemicals liberated by TPP act as a potential allelopathic agent (see also a review by Cembella [20]) affecting the growth, as well as the competitive ability of other toxin-sensitive phytoplankton. At a species-level interaction, these allelopathic effects can ensure a stable coexistence of those nonallelopathic phytoplankton that would otherwise exhibit competitive exclusion [18]. The resultant effects of toxin-allelopathy in species-level interaction thus promote the survival of the weak species belonging to the group of nontoxic phytoplankton (NTP), thereby favoring the diversity of the entire phytoplankton group [18, 19]. Moreover, driven by the fluctuation of the toxin-inhibition effect on zooplankton, the dynamics of a large number of nontoxic and toxic phytoplankton along with grazer zooplankton, when considered as separate groups, switch between oscillations and stability, leading to a planktonic nonequilibrium in a homogeneous environment [17]. Thus, in a homogeneous aquatic environment, TPP generates a twin-interactive effect, namely, toxin-allelopathy due to toxic species on the competing NTP and the inhibitory effects of toxic chemicals on grazer zooplankton, which is potentially responsible for prolonging the coexistence and maintaining biodiversity of phytoplankton and zooplankton species [e.g., 17–19].

Nevertheless, these results have been drawn from the analysis of mathematical models applicable to situations where the species are supposed to experience spatial homogeneity. However, in natural waters, the species of phytoplankton and zooplankton are distributed over a considerably large spatial regime and are prone to spatial movements due to several physical and biological reasons. Species interaction in space and time is a well-known mechanism for the emergence of spatial structure [21, 22]. Applicability of mathematical models to homogeneous nonspatial situations has restricted the scope of the previous models [17, 18] to explore the effect of TPP when the phytoplankton and zooplankton species undergo spatial movements.

The objective of this article is to investigate the effects of spatial interaction on plankton populations in the presence of toxic species. More specifically, the study aims to explore the influence of TPP on the emergence of phytoplankton and zooplankton species over space and time in the subsurface of natural waters. To do this, I proceed in the following two steps: Firstly, I concentrate only on species-level interaction among nontoxic and toxic phytoplankton. Starting from a situation where TPP promotes stable coexistence of NTP in a homogeneous environment, I incorporate the effect of spatial movement and explore the emergence of phytoplankton species in space and time. To a two-nontoxic–one-toxic phytoplankton model that has been originally considered by Roy and Chattopadhyay [18], I incorporate a spatial effect in the form of a one-dimensional

(horizontal) diffusion. The spatiotemporal distribution of the competing species in the presence of toxic phytoplankton is investigated. In the second step, I consider the spatial interaction among NTP, TPP, and zooplankton at the group level. A spatial effect is incorporated, again in the form of a one-dimensional diffusion, to a model originally developed by Roy et al. [17] to describe the interactions at the group level among NTP, TPP, and zooplankton. I explore the emergence of the overall plankton population in space and time as a combination of these three functional groups.

The organization of the paper is as follows. In Section 2, the spatial model of two-nontoxic–one-toxic phytoplankton is analyzed and simulated. In Section 3, the model of NTP–TPP–zooplankton groups is analyzed and simulated. In Section 4, the overall results are discussed in the context of the space–time emergence of phytoplankton and zooplankton species in natural environments.

2 A Reaction-diffusion Model of Two NTP Species and A TPP Species

For describing the spatial interaction among two NTP (say, species 1 with biomass P_1 and species 2 with biomass P_2) and one TPP (say, species 3 with biomass P_T), I formulate a mathematical model in the form of a set of reaction-diffusion equations under the following assumptions:

- The NTP species (species 1 and 2) compete following the Lotka–Volterra competition model, where species 1 is a stronger competitor than species 2.
- Because the TPP species release toxic chemicals, the NTP species can hardly impose any competitive effect on them. Thus, the competitive interaction between a nontoxic and a toxic phytoplankton is negligible [23].
- Allelopathic interactions between a NTP and a TPP are described by a nonlinear function suggested by Solé et al. [23].
- The spatial movement of the species on the water surface is described by a horizontal diffusion term.

Under these assumptions, the reaction-diffusion model can be written as follows:

$$\frac{\partial P_1}{\partial t} = P_1 (r_1 - \alpha_1 P_1 - \beta_{12} P_2 - \gamma_1 P_1 P_T^2) + D_1 \frac{\partial^2 P_1}{\partial x^2}, \quad (1)$$

$$\frac{\partial P_2}{\partial t} = P_2 (r_2 - \alpha_2 P_2 - \beta_{21} P_1 - \gamma_2 P_2 P_T^2) + D_2 \frac{\partial^2 P_2}{\partial x^2}, \quad (2)$$

$$\frac{\partial P_T}{\partial t} = P_T (r_3 - \alpha_3 P_T - \beta_{13} P_1 - \beta_{23} P_2) + D_T \frac{\partial^2 P_T}{\partial x^2}, \quad (3)$$

where $P_1(t, x)$, $P_2(t, x)$, and $P_T(t, x)$, respectively, represent the biomass of the two nontoxic and the toxic phytoplankton at any time t and location x . The meanings of the model parameters and the numerical values considered are given in Table 1. The restrictions on time and space are give by $0 \leq t \leq \infty$ and $-\infty \leq x \leq \infty$, with the following boundary condition inside a boundary $(0, L)$:

$$\frac{\partial P_1(0, t)}{\partial t} = \frac{\partial P_1(L, t)}{\partial t} = \frac{\partial P_2(0, t)}{\partial t} = \frac{\partial P_2(L, t)}{\partial t} = \frac{\partial P_T(0, t)}{\partial t} = \frac{\partial P_T(L, t)}{\partial t} = 0. \quad (4)$$

Table 1 Description and numerical values of parameters of model 1 and model 2 with references

Model	Parameters	Units	Numerical values	Reference
Model 1:	Specific growth rates of	day ⁻¹	0.6, 0.6, 0.66	Roy and
P_1 & P_2 —	P_1, P_2 & P_T (r_1, r_2, r_3)			Chattopadhyay [18]
biomass of	Intraspecific competition	cell ⁻¹ day ⁻¹	0.01, 0.04, 0.06	[18]
two NTP	coefficients ($\alpha_1, \alpha_2, \alpha_3$)			
species, P_T —	Interspecific competition	cell ⁻¹ day ⁻¹	0.02, 0.03,	[18]
biomass of	coefficients ($\beta_{12}, \beta_{21},$		0.005, 0.002	
TPP species	β_{13}, β_{23})			
(cell/lit)	Intensities of allelopathy	cell ⁻³ day ⁻¹	0.00034, 0.00006	[18]
	(γ_1, γ_2)			
	Diffusion coefficients	—	—	Current study
	(D_1, D_2, D_T)			
Model 2:	Specific growth rate of	day ⁻¹	0.4632, 0.4425	Roy et al. [17]
P_N & P_T —	NTP, TPP (r_1, r_2)			
biomass of	Interspecific competition	—	0.002, 0.001	[17]
NTP and	coefficients (α_1, α_2)			
TPP groups,	Phytoplankton carrying	cell lit ⁻¹	505	[17]
Z —biomass of	capacity (K)			
zooplankton	Maximum rates of	day ⁻¹	0.6625, 0.435	[17]
(cell/lit)	predation (w_1, w_2)			
	Half-saturation constants	cell lit ⁻¹	45, 30	[17]
	(m_1, m_2)			
	Maximum NTP conversion	day ⁻¹	0.516	[17]
	rate (ξ_1)			
	Maximum rate of toxin	day ⁻¹	0.198	[17]
	inhibition (ξ_2)			
	Zooplankton mortality (c)	day ⁻¹	0.109	[17]
	Diffusion coefficients	—	—	Current study
	(D_N, D_T, D_Z)			

The model is analyzed under the following initial conditions:

$$P_1(0, x) > 0, P_2(0, x) > 0, P_T(0, x) > 0, \forall x. \quad (5)$$

Analysis of the nonspatial form of the above model (in the absence of diffusion) has been reported in Roy and Chattopadhyay [18], and it has been shown that the model system (1–3) in the absence of diffusion is locally asymptotically stable around the positive interior equilibrium (P_1^*, P_2^*, P_T^*). Now, the solution of the linearized form of the system (1–3) can be written as follows.

$$\begin{pmatrix} P_1 \\ P_2 \\ P_T \end{pmatrix} = \begin{pmatrix} \rho_1 \\ \rho_2 \\ \rho_T \end{pmatrix} \exp(\lambda t) \cos(qx). \quad (6)$$

Here, λ is the rate of time evolution and q is the wave number of the spatial perturbation. Substituting the above solution in the linearized form of the system (1–3) around the positive interior equilibrium (P_1^*, P_2^*, P_T^*), the characteristic equation corresponding to the linearized form of the system (1–3) is obtained as follows:

$$\lambda^3 + R_1 \lambda^2 + R_2 \lambda + R_3 = 0, \quad (7)$$

where

$$R_1 = Q_1 + (D_1 + D_2 + D_T) q^2, \tag{8}$$

$$R_2 = Q_2 + (D_1 D_2 + D_2 D_T + D_1 D_T) q^4 - \left(m_{11} (D_2 + D_T) + m_{22} (D_1 + D_T) + m_{33} (D_1 + D_2) \right) q^2, \tag{9}$$

$$R_3 = Q_3 + D_1 D_2 D_T q^6 + (-D_1 D_2 m_{33} - D_1 m_{22} D_T - m_{11} D_2 D_T) q^4 + (D_1 m_{22} m_{33} + m_{11} m_{22} D_T + m_{11} D_2 m_{33} - m_{21} m_{12} D_T - D_1 m_{23} m_{32} - m_{31} m_{13} D_2) q^2. \tag{10}$$

The quantities Q_1 , Q_2 , and Q_3 are the coefficients of the characteristic equation in the absence of diffusion ($D_1 = D_2 = D_T = 0$), and the Ruth–Hurwitz criterion for the stability of the interior equilibrium in the absence of diffusion implies that $Q_1 > 0$, $Q_3 > 0$, and $Q_1 Q_2 - Q_3 > 0$. The quantities $m_{ij}(i, j = 1, 2, 3)$ are the elements of the community matrix of the model system (1–3) in the absence of diffusion and are given as follows:

$$\left. \begin{aligned} m_{11} &= -P_1^* (\alpha_1 + \gamma_1 (P_T^*)^2) < 0, \\ m_{12} &= -\beta_{12} P_1^* < 0, \\ m_{13} &= -2\gamma_1 P_1^* P_T^* < 0, \\ m_{21} &= -\beta_{21} P_2^* < 0, \\ m_{22} &= -P_2^* (\alpha_2 + \gamma_2 (P_T^*)^2) < 0, \\ m_{23} &= -2\gamma_2 P_2^* P_T^* < 0, \\ m_{31} &= -\beta_{13} P_T^* < 0, \\ m_{32} &= -\beta_{23} P_T^* < 0, \\ m_{33} &= -P_T^* \alpha_3 < 0. \end{aligned} \right\} \tag{11}$$

Here, (P_1^*, P_2^*, P_T^*) is the interior equilibrium of the system (1–3). From the equation of R_3 , I define the following quantities:

$$H_0 = D_1 D_2 D_T, \tag{12}$$

$$H_1 = -D_1 D_2 m_{33} - D_1 m_{22} D_T - m_{11} D_2 D_T, \tag{13}$$

$$H_2 = D_1 m_{22} m_{33} + m_{11} m_{22} D_T + m_{11} D_2 m_{33} - m_{21} m_{12} D_T - D_1 m_{23} m_{32} - m_{31} m_{13} D_2. \tag{14}$$

Some algebraic manipulations show that at least one root of the equation (7) has a positive real part, and thus, diffusive instability (Turing) occurs if either $(H_2 < 0)$ or $(H_1 < 0$ and $H_1^2 > 3 H_0 H_2)$. If any of the above conditions are satisfied, the minimum value of the wave number q for which Turing instability occurs is given by the following:

$$q_{\min} = \sqrt{(1/(3 H_0)) \left(-H_1 + \sqrt{H_1^2 - 3 H_0 H_2} \right)}. \tag{15}$$

However, for the model system (1–3) $H_2 > 0$ and $H_1 > 0$, and thus, no sufficient condition exists for the emergence of Turing instability for this system.

It is well known that the traditional Turing pattern might be expected only under the assumption that the diffusivities of the species are unequal [21]. However, because the dispersals of the species in a planktonic system are due to turbulent mixing, an assumption

of unequal diffusivity might be unlikely. Moreover, Turing instability results in stationary and regular patterns, whereas, in a real-world plankton community, the spatial patterns observed are nonstationary and irregular [7, 24]. Following these observations, it is fair to investigate the dynamics of NTP–TPP species under equal diffusivity assumptions ($D_1 = D_2 = D_T = D$, say).

The behavior of a reaction-diffusion system is expected to depend on the choice of initial conditions. A purely homogeneous initial condition may hardly generate any non-Turing spatial pattern under equal diffusivity [7]. In such cases, the system maintains its homogeneity over space and the densities of the variables approach attractors [25]. From a biological or physical point of view, it is reasonable to assume that, instead of a purely homogeneous distribution, the species are scattered nonuniformly over the space under consideration [7, 25]. For the subsequent simulations of the model, the initial distribution of the species over the space has been taken to be uniform. The scattered distribution of the populations over the space has been initiated by a random sampling of the species biomass around the equilibrium values of the corresponding nonspatial models. These samples were used to initialize the biomass over the whole space grids. Further, the biomass distribution of the species has been initially assigned constant equal values over the times step at the two end points of the spatial grids.

The spatial model (1–3) simulated at different equal diffusivity conditions gives rise to characteristically different spatiotemporal biomass pattern for the three phytoplankton

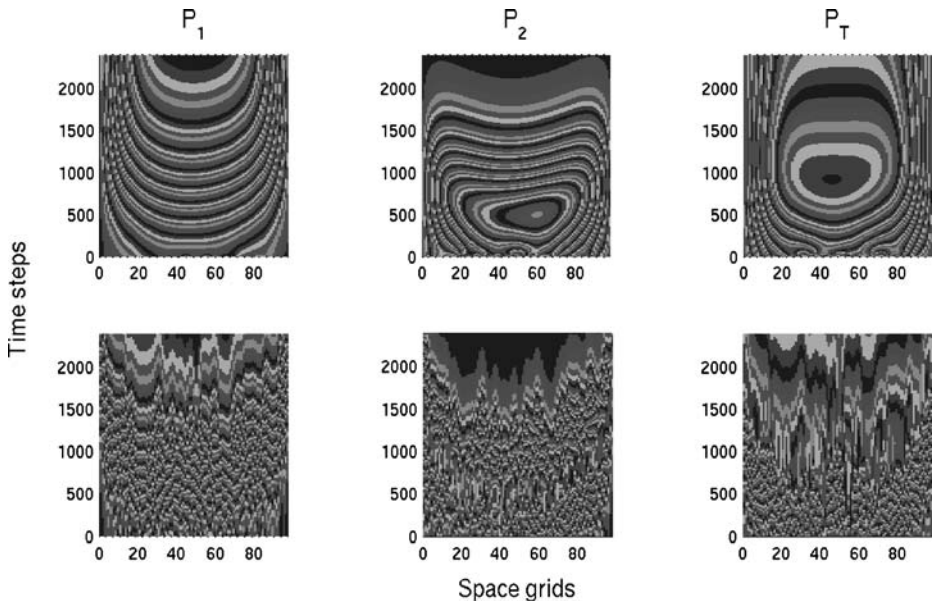


Fig. 1 Patchy pattern of biomass distribution over space and time of two NTP and a TPP obtained from the model system (1–3). Parameters of the model are given in Table 1. Two characteristically different patches are obtained for two different values of the equal diffusivity. The *upper panels* are simulation results for NTP species 1, NTP species 2, and the TPP species for equal diffusivity $D_1 = D_2 = D_T = D = 1.25$. The *lower panels* are obtained for the same species for equal diffusivity $D_1 = D_2 = D_T = D = 0.005$. The space grids are of 0.2 unit and the time steps are of 0.005 unit

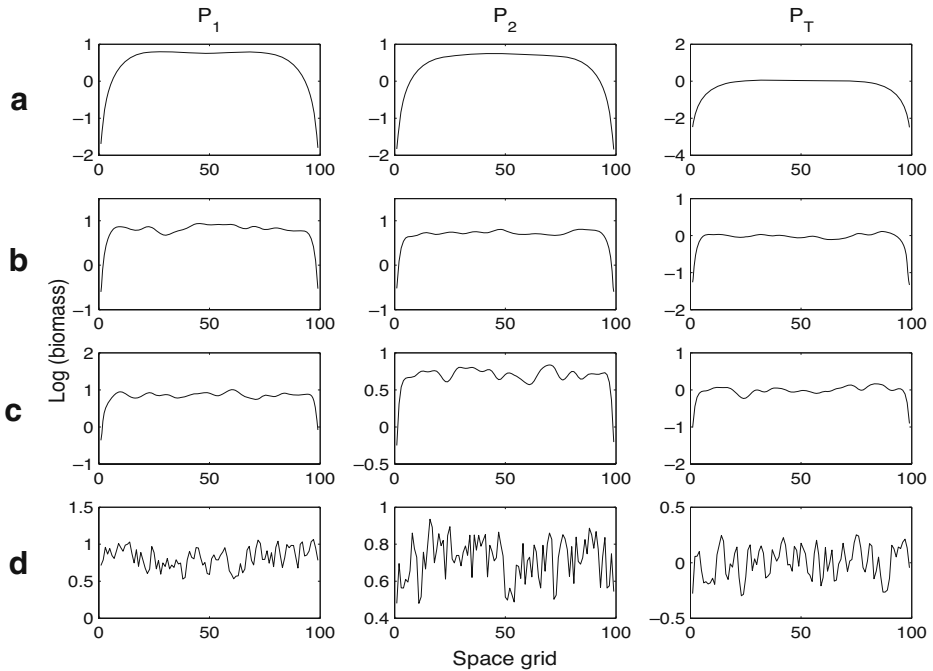


Fig. 2 Spatial distribution of two NTP species (P_1 and P_2) and a TPP species (P_T) described by model system (1–3) at equal diffusivities ($D_1 = D_2 = D_T = D$). Keeping the initial condition the same corresponding to each value of D , the spatial distributions of P_1 , P_2 , and P_T at time step 400 (time steps are of 0.005 unit) are presented in *left, middle, and right panels* respectively. Each *row* represents the spatial distributions at a given diffusivity: **a** $D = 1.25$, **b** $D = 0.09$, **c** $D = 0.05$, **d** $D = 0.005$

species. At a high diffusivity $D = 1.25$, the visible spatiotemporal patches of the individual species of NTP and TPP emerge over the space–time plane (Fig. 1, upper panels). However, the inhomogeneous patchy pattern of the biomass distribution of competing NTP along with TPP changes with variations in diffusivity. The spatial patches shrink and become characteristically irregular for a low diffusivity $D = 0.005$ (Fig. 1, lower panels). With a gradual decrease in diffusivity, the biomass distribution of the species remains spatially irregular (Fig. 2). For a given initial condition, the species exhibits a spatial distribution almost regular and wavy at high diffusivity ($D = 1.25$), but highly irregular and fluctuating at a sufficiently low diffusivity ($D = 0.005$) (Fig. 2). The coefficient of variation (which is the ratio of standard deviation to mean) of the species biomass at any time point over space also explains the variation of the species distribution for different diffusivity (Fig. 3). While the initial distribution in these simulations was such that the biomass was random over the spatial grid, a high strength of the diffusivity supports the formation of visible patches from out of the random biomass distribution.

The dominance level of the two NTPs (P_1 and P_2) varies in space and time. For a nonspatial interaction, P_1 dominates P_2 for the fixed parameter values considered, which leads to a complete exclusion of P_2 in the absence of the toxic species P_T [18]. However, due to spatial movements, the dominance level shows complexity over space and time (Fig. 4). For high diffusivity ($D = 1.25$), the space–time plane is divided into a number of

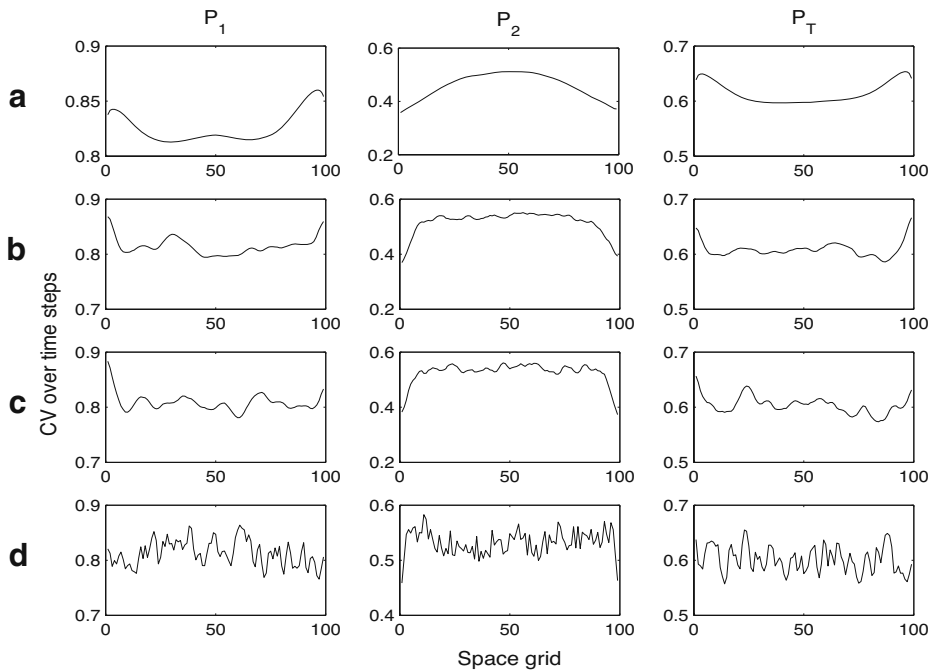


Fig. 3 The spatial distribution of the coefficient of variation (CV), which is the ratio of standard deviation to mean of biomass over time for NTP species 1, NTP species 2, and the TPP species. Each row represents the spatial distributions at a given diffusivity: **a** $D = 1.25$, **b** $D = 0.09$, **c** $D = 0.05$, **d** $D = 0.005$

regions such that either P_1 or P_2 dominates in each region (Fig. 4a–b). For low diffusivity ($D = 0.005$), these regions shrink and form a large number of narrow stripe-like regions of irregular area such that any of the species P_1 or P_2 dominates in each such stripe (Fig. 4c–d). These results suggest that, in the presence of toxic species, the intensity of diffusion determines the dominance level of the species over space and time coordinates.

As mentioned before, in a homogeneous medium, a system of competing phytoplankton exhibits stable coexistence due to the presence of toxic phytoplankton [18]. Simulations here suggest that, if the overall interaction takes place in space and time, which is natural for real-world plankton populations, the species distribution is relatively complex. A variation in the diffusivity, which the modulation in the inhomogeneous patch structure on the water surface is responsible for, may be driven by several physical forces. The results show that the biomass distribution in space and time of those phytoplankton systems consisting of TPP and NTP strongly depends of the rate of their spatial movements, and a spatial nonhomogeneous biomass emerges over certain space–time grids. In other words, the toxin-allelopathy pulls towards dynamical stability, whereas the heterogeneity of the biomass distribution over space is governed by the diffusion process caused by factors related to physical forcing.

Now, when the overall plankton community is considered, the effects of the predator zooplankton play a crucial role on the dynamics of the competing phytoplankton species. In the following section, I investigate the role of diffusion on the interacting groups of phytoplankton distinguished as nontoxic and toxic in the presence of common grazers, zooplankton.

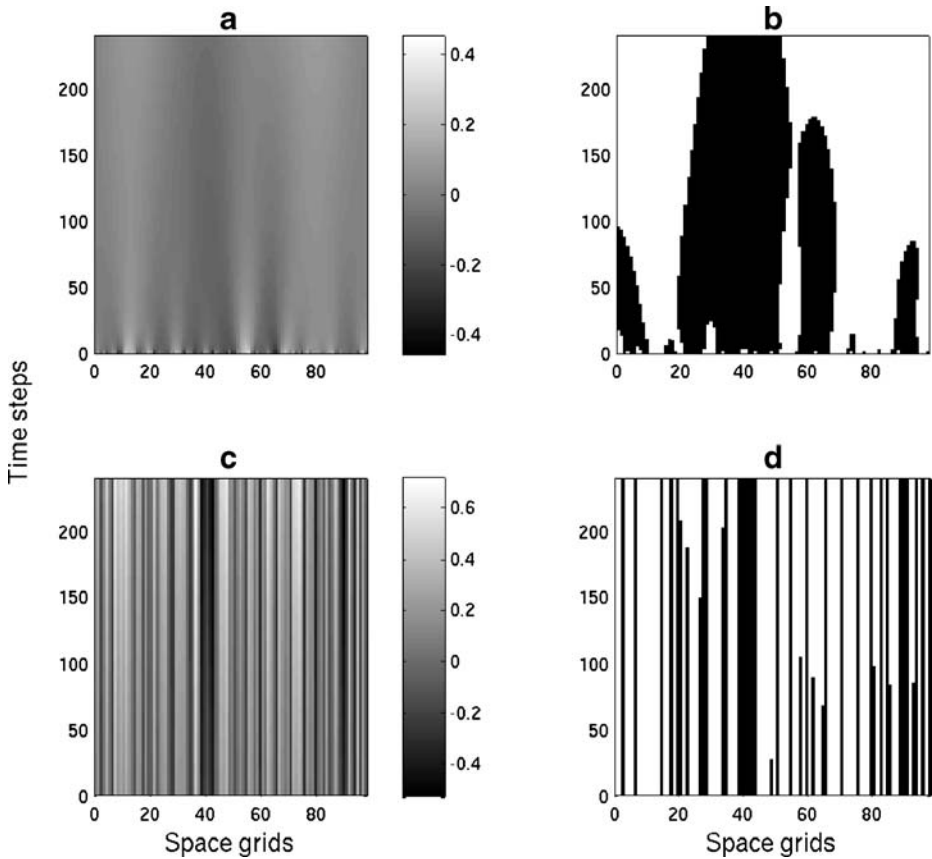


Fig. 4 Level of dominance of two NTP species over space and time. All the figures are obtained at a common initial condition; the upper panels (**a** and **b**) at equal diffusivity $D = 1.25$, and the lower panels (**c** and **d**) at $D = 0.005$. The left panels (**a** and **c**) represent the levels of difference in the biomass of P_1 and P_2 ($P_1 - P_2$) over space and time. The right panels (**b** and **d**) depict the space and time at which either P_1 or P_2 is dominant; the *white shades* stand for P_1 dominance and *black shades* stand for P_2 dominance

3 A Reaction-diffusion Model of NTP, TPP, and Zooplankton Groups

I formulate a mathematical model describing the spatial interaction of three groups of plankton (namely, NTP, TPP, and zooplankton) under the following assumptions:

- NTP and TPP population follow logistic growth in the absence of the grazer [26].
- Both groups of phytoplankton exhibit a Holling type-II functional response to the grazer zooplankton.
- Toxic materials ingested on predation of TPP result in a significant inhibitory effect on zooplankton growth. It has been shown that the inhibitory substances released by TPP reduce the grazing pressure of zooplankton [e.g., 27]. Further, field studies have shown that micro- and mesozooplankton populations are reduced during the blooms of a chrysophyte *Aureococcus anophagefferens* [28]. Although this negative effect of TPP on zooplankton is well known, the exact functional form describing the reduction

of zooplankton grazing due to TPP biomass is still unknown. However, in Roy et al. [17], the effect of TPP on zooplankton has been modelled mechanistically through a negative Holling type II function, and the overall dynamics has been shown consistent with a set of field observations. In the following, the effect of TPP on zooplankton in a homogeneous media is described by the model proposed by Roy et al. [17].

- (d) The spatial movement of the species on the water surface is described by a horizontal diffusion term.

Under these assumptions, the mathematical model can be written as follows:

$$\frac{\partial P_N}{\partial t} = P_N \left\{ r_1 \left(1 - \frac{P_N + \alpha_1 P_T}{K} \right) - \frac{w_1 Z}{m_1 + P_N} \right\} + D_N \frac{\partial^2 P_N}{\partial x^2}, \quad (16)$$

$$\frac{\partial P_T}{\partial t} = P_T \left\{ r_2 \left(1 - \frac{P_T + \alpha_2 P_N}{K} \right) - \frac{w_2 Z}{m_2 + P_T} \right\} + D_T \frac{\partial^2 P_T}{\partial x^2}, \quad (17)$$

$$\frac{\partial Z}{\partial t} = Z \left\{ \frac{\xi_1 P_N}{m_1 + P_N} - \frac{\xi_2 P_T}{m_2 + P_T} - c \right\} + D_Z \frac{\partial^2 Z}{\partial x^2}. \quad (18)$$

Here, $P_N(t, x)$, $P_T(t, x)$, and $Z(t, x)$ represent, respectively, the biomass at any time t and location x of the NTP, TPP, and zooplankton groups. The parameters of the model are described in Table 1. The restrictions on time and space are given by $0 \leq t \leq \infty$ and $-\infty \leq x \leq \infty$. Again, the following boundary condition is assumed inside a boundary $(0, L)$,

$$\frac{\partial P_N(0, t)}{\partial t} = \frac{\partial P_N(L, t)}{\partial t} = \frac{\partial P_T(0, t)}{\partial t} = \frac{\partial P_T(L, t)}{\partial t} = \frac{\partial Z(0, t)}{\partial t} = \frac{\partial Z(L, t)}{\partial t} = 0. \quad (19)$$

The model is analyzed under the following initial conditions:

$$P_N(0, x) > 0, \quad P_T(0, x) > 0, \quad Z(0, x) > 0, \quad \forall x. \quad (20)$$

Analysis of the nonspatial form of the above model, i.e., in the absence of diffusion, has been reported in Roy et al. [17], and it has been shown that under the parameter set considered in Table 1 the system is locally asymptotically stable around the interior equilibrium (P_N^*, P_T^*, Z^*) . Following that study, for the model system (16–18), the elements of the community matrix around the interior equilibrium (P_N^*, P_T^*, Z^*) in the absence of diffusion are obtained as follows:

$$\left. \begin{aligned} m_{11} &= P_N^* \left(-r_1/K + w_1 Z^*/(m_1 + P_N^*)^2 \right) < 0, \\ m_{12} &= -\alpha_1 r_1 P_N^*/K < 0, \\ m_{13} &= -w_1 P_N^*/(m_1 + P_N^*) < 0, \\ m_{21} &= -\alpha_2 r_2 P_T^*/K < 0, \\ m_{22} &= P_T^* \left(-r_2/K + w_2 Z^*/(m_2 + P_T^*)^2 \right) < 0, \\ m_{23} &= -w_2 P_T^*/(m_2 + P_T^*) < 0, \\ m_{31} &= \xi_1 m_1 Z^*/(m_1 + P_N^*)^2 > 0, \\ m_{32} &= -\xi_2 m_2 Z^*/(m_2 + P_T^*)^2 < 0, \\ m_{33} &= 0. \end{aligned} \right\} \quad (21)$$

Again, with the symbols having meanings defined previously in the case of model system (1–3), for the model system (16–18), $H_1 > 0$. Now, a set of sufficient conditions for

$H_2 < 0$, and thus, for diffusion-driven instability (Turing) around the interior equilibria (P_N^*, P_T^*, Z^*) , is the following:

$$\begin{aligned}
 &P_N^* P_T^* [-r_1 + (w_1 Z^* K)/(m_1 + P_N^*)^2] \times [-r_2 + (w_2 Z^* K)/(m_2 + P_T^*)^2] D_Z \\
 &+ (\xi_1 w_1^2 P_N^* Z^* D_T)/(m_1 + P_N^*)^3 < (\alpha_1 r_1 \alpha_2 r_2 P_N^* P_T^*) D_Z / K^2 \quad (22) \\
 &+ (\xi_2 w_2^2 P_T^* Z^* D_N)/(m_2 + P_T^*)^3.
 \end{aligned}$$

The model (16–18) is simulated using the parameter values considered in Table 1, which were originally estimated by Roy et al. [17] using a set of field-collected samples. Suitable choices of the diffusivities (D_N , D_T , and D_Z) lead to the emergence of Turing patterns for the biomass distribution of NTP, TPP, and zooplankton populations (Fig. 5). This result suggests that, when the spatial movements of NTP, TPP, and zooplankton groups occur with unequal diffusivities, an inhomogeneous spatial pattern (Turing) emerges.

As argued in the previous section, the spatial diffusivities of different species in a planktonic system are very likely to be equal in magnitude. However, since the movement of zooplankton is generally governed by their swimming activities, it is reasonable to assume

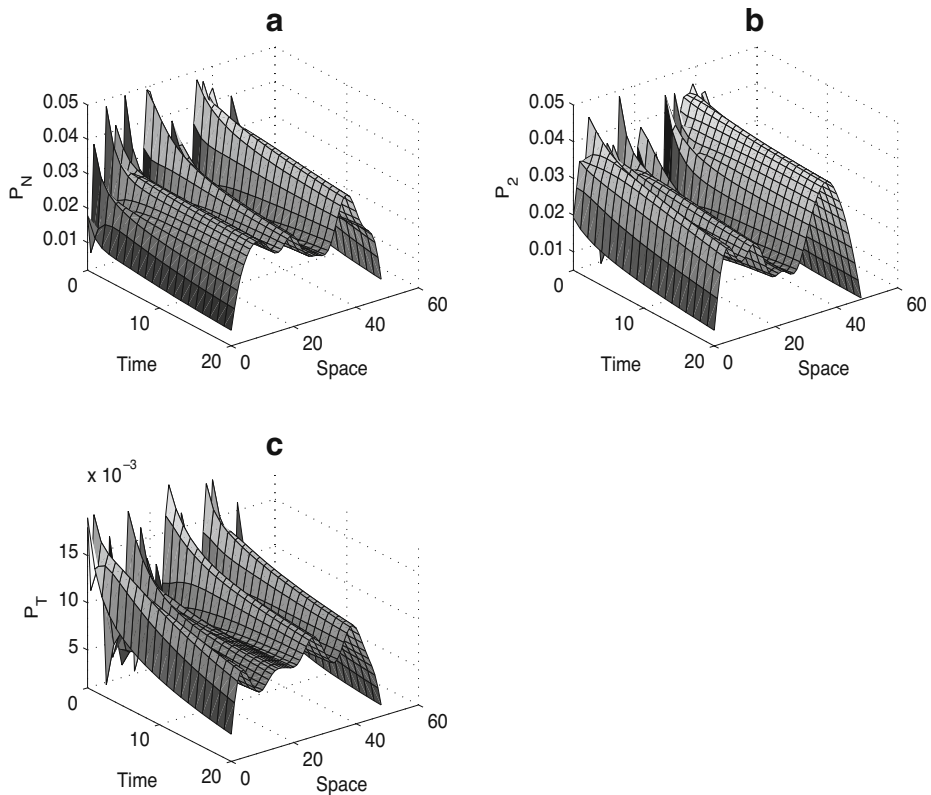


Fig. 5 Turing instability corresponding to the model system (16–18). The parameters are fixed at the values given in Table 1, and an appropriate arbitrary values for the diffusions coefficient are chosen ($D_1 = 5 \times 10^4$, $D_2 = 0.5 \times 10^{-7}$, $D_Z = 1 \times 10^{-5}$) that satisfy the sufficient condition for diffusive instability given in (20). Turing pattern is shown for **a** NTP group (P_N), **b** TPP group (P_T), and **c** zooplankton group (Z)

that their diffusion coefficient is higher than that of phytoplankton. In other words, due to swimming activity, D_Z is likely to be higher than D_N and D_T by an order of magnitude. The spatial emergence of the species biomass under these two conditions, namely, equal diffusivity and higher zooplankton diffusivity, is, therefore, very likely to be different. Under an equal diffusivity ($D_N = D_T = D_Z = D = 0.5$, say) assumption, for the set of parameters fixed as in Table 1, a spatially inhomogeneous distribution of NTP, TPP, and zooplankton biomass emerges (Fig. 6, upper panels): all three groups of plankton species coexist over time and space. However, when the diffusivity of zooplankton is considered higher than that of phytoplankton by an order of magnitude ($D_N = 0.00125$, $D_T = 0.00125$, $D_Z = 1.25$), the pattern of biomass distributions of phytoplankton and zooplankton that emerged over space and time is characteristically different, both from each other (Fig. 6, lower panels) and from that which emerged under equal diffusivity (Fig. 6). Zooplankton, which is a common grazer of NTP and TPP, benefits from predation of NTP but is affected on ingestion of TPP [17]. The distribution of zooplankton biomass over space and time is thus regulated by a combined effect of NTP and TPP presence. For equal diffusivity ($D = 0.5$), zooplankton biomass forms visible patches distributed over space and time, and the distribution of biomass NTP and TPP forms visible patches (Fig. 6). On the other hand, for high diffusivity of zooplankton, although the biomass distribution of zooplankton forms visible regular patches, the biomass distributions of NTP and TPP form irregular patterns (Fig. 6).

The total phytoplankton biomass, in this case, is a combination of the biomass of NTP and TPP groups, and the difference between these two groups determines the dominance of

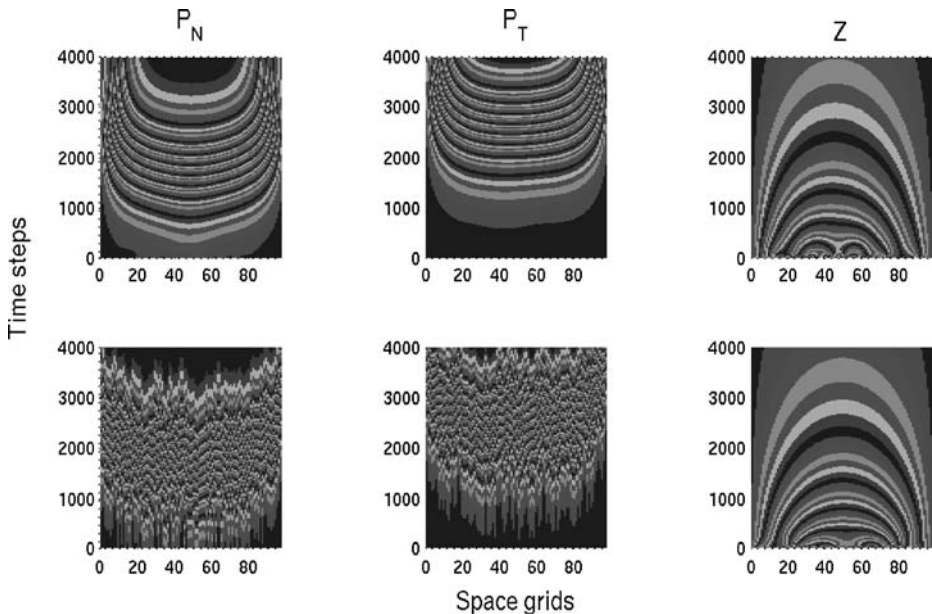


Fig. 6 Patchy pattern of biomass distribution over space and time of the two phytoplankton groups (NTP, TPP) and the zooplankton group obtained from the model system (16–18). Parameters of the model are given in Table 1. The patches in the *upper panels* are obtained for equal diffusivity $D_1 = D_2 = D_T = D = 0.5$. The patches in the *lower panels* are obtained for high zooplankton diffusivity $D_N = D_T = 0.00125$, $D_Z = D = 1.25$. The space grids are of 0.2 unit and the time steps are of 0.005 unit

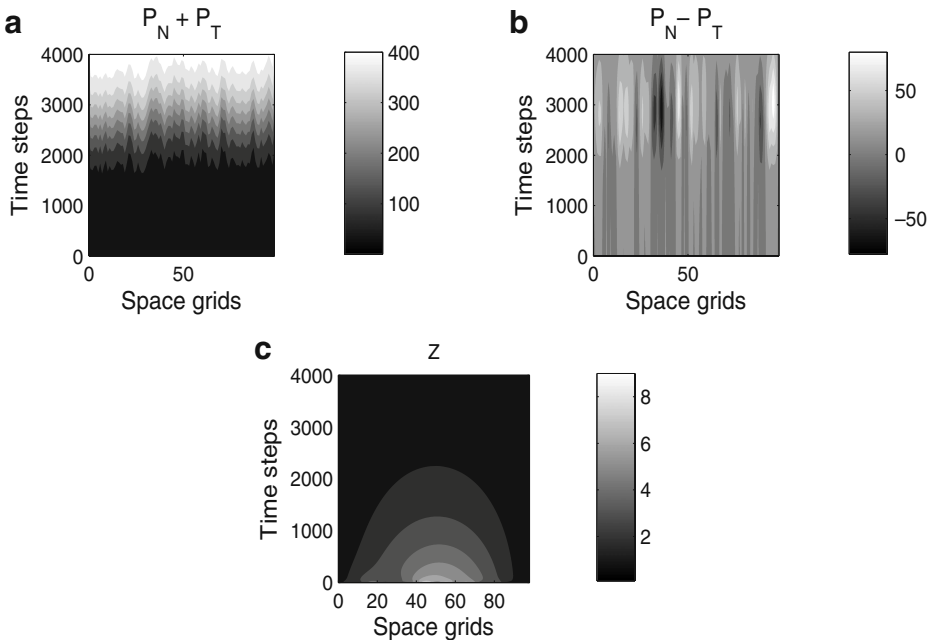


Fig. 7 Distribution of biomass level over space and time for **a** the total phytoplankton NTP+TPP, **b** the difference of the NTP and TPP populations (NTP–TPP), and **c** the zooplankton population. Parameters of the model are given in Table 1. The distributions are obtained for $D_N = D_T = 0.00125$, $D_Z = D = 1.25$. The biomass distributions in panels **a**, **b**, and **c** over time and space depict different patterns

either NTP or TPP. For high diffusivity of zooplankton, the total phytoplankton biomass, the biomass difference between NTP and TPP, and the zooplankton biomass form inhomogeneous patches visibly distributed over space and time (Fig. 7a–c). However, the distributions are characteristically different from each other. Over a time scale, the distribution of the total phytoplankton emerges in a similar pattern (Fig. 7a), and the patches of zooplankton distribution are also regular (Fig. 7c). On the other hand, the biomass-distribution pattern of the difference between NTP and TPP changes over time steps (Fig. 7b). This distribution shows that the densities of the toxic species and the nontoxic species over spatial locations change over time, which leads to the emergence of toxic patches and nontoxic patches (Fig. 7b). The presence of TPP at different densities in different patches determines the distribution of zooplankton biomass (due to inhibitory effects), and the zooplankton in turn regulate the distribution of NTP biomass (due to faster spatial movement) over space and time. The overall distribution may be visibly patchy, or even spatially irregular. These results demonstrate that, due to spatial interaction, the emergence of NTP and zooplankton groups in the presence of the TPP group is possible in inhomogeneous biomass distributed over space and time.

4 Discussion

Recent studies have highlighted the role of toxin-producing species of phytoplankton on the dynamics of phytoplankton–zooplankton interactions [16, 19, 29–31]. Some previous

reports [17–19] have suggested that the presence of TPP might provide a potential mechanism for the maintenance of the coexistence and biodiversity of many phytoplankton and zooplankton species in a homogeneous environment. Here, I demonstrate how a nonhomogeneous biomass distribution of competing phytoplankton and grazer zooplankton emerges over space and time in the presence of toxic species. The study demonstrates that, in the absence of grazer zooplankton, through a spatial interaction among nontoxic and toxic phytoplankton, a non-Turing spatial pattern emerges. The spatial structure of inhomogeneous biomass distribution of NTP and TPP species on the water surface depends on the diffusion coefficients. These patches are distributed over the space in such a manner that the dominance level of each species has a distinct demarcation from that of the other. In the presence of TPP, these spatial structures are obtained under parameter conditions that lead to a competitive exclusion of weak species when TPP is absent. Spatial heterogeneity generated due to spatial interaction among nontoxic and toxic phytoplankton thus ensures the emergence of multiple species over space and time. On the other hand, spatial interaction among the groups of NTP, TPP, and zooplankton under suitable conditions exhibits Turing patterns and, under equal-diffusivity assumptions, generates non-Turing patterns. Similar to species-level interaction, the inhomogeneous patch formations of total phytoplankton and zooplankton groups are also dependent on the diffusion coefficients. The distribution of the zooplankton species in space–time regulated by the biomass distribution of toxic species determines in turn the biomass of the total phytoplankton. Thus, in the presence of the TPP group, interaction among the phytoplankton and zooplankton groups exhibits spatial heterogeneity, thereby maintaining the biodiversity.

In natural waters, the dynamics of phytoplankton and zooplankton is regulated by a huge number of physical and biological factors. Generation of inhomogeneous patchy distribution of plankton species on the water surface may really be a result of all such factors, making it very difficult to incorporate each and every one in a model (see also, Medvinsky et al. [7]). The present study has concentrated solely on direct interactions among many phytoplankton species structured as NTP and TPP, along with the grazer zooplankton. The mechanisms evolved for the space–time survival of these species are thus regulated by interspecific spatial interaction. The role of TPP is significant in this context. It has been established earlier that TPP acts as a stabilizing factor for phytoplankton–phytoplankton and phytoplankton–zooplankton interaction [17, 18]. The present study suggests that, on one hand, TPP species pull towards dynamic stability, and on the other hand, spatial movement leads towards spatial instability, resulting in the emergence of phytoplankton and zooplankton species in inhomogeneous biomass distributions over space and time. Thus, the species of the TPP group present within the plankton community itself can be viewed as a potential self-regulating candidate, which, combined with physical movement of the plankton species and the structure of the biomass distribution, boosts the emergence of the species in the subsurface water.

In a number of previous studies, self-organized patchiness and spatiotemporal chaos in predator–prey systems (with apparent application to plankton dynamics) have been reported [e.g., 7, 24, 32]. On one hand, the results of the present study potentially give an extension of the conceptual results of those studies onto a three-species model plankton system. On the other hand, this study extends onto a space–time frame the rather newly introduced mechanism for promotion of plankton diversity due to the presence of TPP [see 6, 19]. To further extrapolate the results of this study, a couple of complimentary extensions might be worth investigating. Firstly, the spatial movement considered here is horizontal and, thus, one-dimensional; however, the movements of the plankton species in the real world are

three-dimensional. So, it might be of interest to verify the role of TPP species under three-dimensional movement of the species. Finally, to avoid the model-specificity of the results, a number of other interaction models (e.g., nutrient–phytoplankton–zooplankton models) might be considered for the investigation of the effects of TPP under spatial interactions.

Acknowledgements The present research of S. Roy is supported by a Royal Society International Fellowship. The valuable comments of Professor K. J. Flynn, University of Swansea, on an early version of the paper are acknowledged. The author thanks the learned referees for their valuable comments that have improved the presentation of the paper.

References

- Hutchinson, G.E.: The paradox of the plankton. *Am. Nat.* **95**, 137–145 (1961)
- Richerson, P.J., Armstrong, R., Goldman, C.R.: Contemporaneous disequilibrium: a new hypothesis to explain the paradox of plankton. *Proc. Natl. Acad. Sci. U. S. A.* **67**, 1710–1714 (1970)
- Huisman, J., Weissing, F.J.: Biodiversity of plankton by species oscillation and chaos. *Nature* **402**, 407–410 (1999)
- Huisman, J., Pham Thi, N.N., Karl, D.M., Sommeijer, B.: Reduced mixing generates oscillations and chaos in the oceanic deep chlorophyll maximum. *Nature* **439**, 322–325 (2006)
- Scheffer, M., Rinaldi, S., Huisman, J., Weissing, F.J.: Why phytoplankton communities have no equilibrium: solutions to the paradox. *Hydrobiologia* **491**, 9–18 (2003)
- Roy, S., Chattopadhyay, J.: Towards a resolution of the paradox of the plankton: a brief overview of the existing mechanisms. *Ecol. Complex.* **4**(1–2), 26–33 (2007)
- Medvinsky, A.B., Petrovskii, S.V., Tikhonova, I.A., Malchow, H., Li, B.L.: Spatiotemporal complexity of plankton and fish dynamics. *SIAM Rev.* **44**, 311–370 (2002)
- Hallam, T., Clark, C., Jordan, G.: Effects of toxicants on populations: a qualitative approach. II. First order kinetics. *J. Theor. Biol.* **18**, 25–37 (1983)
- Arzul, G., Seguel, M., Guzman, L., Denn, E.E.-L.: Comparison of allelopathic properties in three toxic alexandrium species. *J. Exp. Mar. Biol. Ecol.* **232**(C11), 285–295 (1999)
- Chan, A., Andersen, R., Blanc, M.L., Harrison, P.: Algal planting as a tool for investigating allelopathy among marine microalgae. *Mar. Biol.* **84**, 287–291 (1980)
- Nielsen, T.G., Kjørboe, T., Bjørnsen, P.K.: Effects of a *Chrysochromulina polylepis* subsurface bloom on the plankton community. *Mar. Ecol. Prog. Ser.* **62**, 21–35 (1990)
- Schmidt, L., Hansen, P.: Allelopathy in the prymnesiophyte *Chrysochromulina polylepis*: effect of cell concentration, growth phase and pH. *Mar. Ecol. Prog. Ser.* **216**, 67–81 (2001)
- Fistarol, G., Legrand, C., Graneli, E.: Allelopathic effect of *primesium parvum* on a natural plankton community. *Mar. Ecol. Prog. Ser.* **255**, 115–125 (2003)
- Fistarol, G., Legrand, C., Selander, E., Hummert, C., Stolte, W., Graneli, E.: Allelopathy in alexandrium spp.: effect on a natural plankton community and on algal monocultures. *Aquat. Microb. Ecol.* **35**, 45–56 (2004)
- Kozłowski-Suzuki, B., et al.: Feeding, reproduction and toxin accumulation by the copepods *Acartia bifilosa* and *Eurytenora affinis* in the presence of the toxic cyanobacterium *Nodularia Spumigena*. *Mar. Ecol. Prog.* **249**, 237–249 (2003)
- Chattopadhyay, J., Sarkar, R.R., Mandal, S.: Toxin-producing plankton may act as a biological control for planktonic blooms – field study and mathematical modeling. *J. Theor. Biol.* **215**, 333–344 (2002)
- Roy, S., Alam, S., Chattopadhyay, J.: Competing effects of toxin-producing phytoplankton on the overall plankton populations in the Bay of Bengal. *Bull. Math. Biol.* **68**(8), 2303–2320 (2006)
- Roy, S., Chattopadhyay, J.: Toxin-allelopathy among phytoplankton species prevents competitive exclusion. *J. Biol. Syst.* **15**(1), 73–93 (2007)
- Roy, S., Bhattacharya, S., Das, P., Chattopadhyay, J.: Interaction among nontoxic phytoplankton, toxic phytoplankton and zooplankton: inferences from field observations. *J. Biol. Phys.* **33**(1), 1–17 (2007)
- Cembella, A.D.: Chemical ecology of eukaryotic microalgae in marine ecosystems. *Phycologia* **42**(4), 420–447 (2003)
- Murray, J.D.: *Mathematical Biology*. Springer, Berlin (1989)
- Okubo, A.: *Diffusion and Ecological Problems: Mathematical Models*. Springer, Berlin (1980)

23. Solé, J., García-Ladona, E., Ruardij, P., Estrada, M.: Modelling allelopathy among marine algae. *Ecol. Model.* **183**, 373–384 (2005)
24. Petrovskii, S.V., Malchow, H.: Wave of chaos: new mechanism for pattern formation in spatiotemporal population dynamics. *Theor. Popul. Biol.* **59**, 157–174 (2001)
25. Petrovskii, S.V., Malchow, H.: A minimal model for pattern formation in a prey-predator system. *Math. Comput. Model.* **29**, 49–63 (1999)
26. Odum, E.P.: *Fundamentals of Ecology*. Saunders, Philadelphia (1971)
27. Kirk, K., Gilbert, J.: Variation in herbivore response to chemical defence: zooplankton foraging on toxic cyanobacteria. *Ecology* **73**, 2208 (1992)
28. Buskley, E.J., Stockwell, A.J.: Effect of persistent brown tide on zooplankton population in the Laguna Madre of southern Texas. In: Smayda, T.J., Shimuzu, Y. (eds.) *Toxic Phytoplankton Bloom in the Sea*. Elsevier, Amsterdam, pp. 659–666 (1997)
29. Chattopadhyay, J., Sarkar, R.R., Elabdllaoui, A.: A delay differential equation model on harmful algal blooms in the presence of toxic substances. *IMA J. Math. Appl. Med. Biol.* **19**, 137–161 (2002)
30. Irigoien, X., Flynn, K.J., Harris, R.P.: Phytoplankton blooms: a loophole in microzooplankton grazing impact? *J. Plankton Res.* **27**, 313–321 (2005). doi:[10.1093/plankt/fbi011](https://doi.org/10.1093/plankt/fbi011)
31. Mitra, A., Flynn, K.J.: Promotion of harmful algal blooms by zooplankton predatory activity. *Biol. Lett.* **2**, 194–197 (2006). doi:[10.1098/rsbl.2006.0447](https://doi.org/10.1098/rsbl.2006.0447)
32. Pascual, M.: Diffusion induced chaos in a spatial predator-prey system. *Proc. R. Soc. Lond. Ser. B* **251**, 1–7 (1993)